

Influence of the initial temperature difference between two spaces and different wind flows on the sealing efficiency of an air curtain

Nuno Rafael Vilar Vasques da Costa Mendes

nuno.costa.mendes@tecnico.ulisboa.pt

Instituto Superior Técnico, Universidade de Lisboa – Portugal

January 2021

Abstract

The use of air curtains has been increasing in the last years. They bring several advantages to companies and businesses (energy savings, air quality, safety and thermal comfort). Since their efficiency is influenced by several parameters, such as temperature difference between spaces and the presence of wind, studying the influence of such parameters on air curtain efficiency is paramount. The objective of this study was to separately calculate the efficiency trends of an air curtain subjected to distinct initial temperature differences and wind flows. 2D and 3D CFD simulations, using the turbulence model $k-\varepsilon$ Realizable, were conducted. These were based on Eurovent recommendations on air curtain testing. On distinct temperature differences, the 3D results showed that, as the initial temperature difference increases, AC efficiency increases. However, the 2D results showed an opposite trend. For distinct wind flows, both 2D and 3D results showed that, as wind flows are increased, AC efficiency decreases. Moreover, since literature is scarce when comparing 2D and 3D simulations, these were comparatively analysed. Although 2D simulations modelled the AC jet correctly, it was concluded that they are not reliable.

Keywords: Air Curtain, Sealing Efficiency, Heat Transfer, CFD, Parametric Study

1. Introduction

Air curtains (ACs) devices create an air barrier between two spaces, restricting heat and mass transfer between them. They were initially created by Theophilus Van Kannel [1], in 1904, and, since then, are used more and more often worldwide. Just in Europe, air curtains represent a €600 million market, which is growing steadily during the last decade [2].

Air curtains have several advantages. By restricting heat and mass transfer between spaces, they provide thermal comfort to workers or costumers. They also promote the quality of the air inside, reducing respiratory illnesses. They inhibit the formation of ice in refrigeration rooms, which can lead to accidents, and, as such, contribute to workers and equipment's safety. Furthermore, they operate at low costs when compared with its competing counterparts, namely air conditioning devices. As such, they decrease energy consumption and, consequently, carbon dioxide (CO₂) emissions, making them an attractive option for companies and industries. They are a versatile technology, having several applications and being used in various places:

public places with an open-door policy, industrial environments, refrigeration rooms, among others. Their versatility, size, low maintenance and low operating costs, gives them a great advantage when compared to other options, such as the abovementioned air conditioning devices, as well as vestibules, polyvinyl chloride (PVC) strips or automated doors.

Since air curtains are proving to be increasingly useful and more and more widespread, several studies have been conducted in the last years to evaluate the performance of these devices when subjected to different conditions.

These were first performed in the 1960s. The work by Takahashi and Inoh (1963) [3] proved to be decisive since it concluded that air curtain devices (ACDs) can reduce the heat transfer between spaces up to 80%. Later, in 1969, Hayes and Stoecker (1969a and 1969b) [4] and [5], proposed the use of a new variable, called deflection modulus (Dm), which allowed to compute the minimum jet velocity needed to create an uninterrupted barrier between the spaces.

Since then, other studies have been conducted. On the last years, these have been focusing on the parameters that influence the performance of an air curtain. These include the initial velocity and orientation of the jet produced by the ACD, the location where the ACD is installed, external conditions, such as the temperature difference between spaces, presence and magnitude of wind flow, and others.

The velocity of the jet is known to be one of the most important parameters influencing the performance of an air curtain. It was studied by Costa *et al.* (2006) [6] and Paepe (2010) [7], who concluded that there is an optimal velocity for a given situation. The use of lower velocities leads to the breakage of the jet and the use of higher velocities facilitates the mixture of air between spaces, leading to a decrease in the efficiency of the AC. Another important factor is the orientation of the jet (Jaramillo *et al.* (2009) [8] and Gonçalves *et al.* (2019) [9]). The literature recommends the use of jets directed to the warm space (0-15° degree angles), to counter the effect of the mass of warm air leaving the warm space in the upper region of the opening (natural convection).

The location of the ACD also influences its performance. Authors like Jaramillo *et al.* (2009) [8] and Gonçalves *et al.* (2012a) [10], concluded that installing the AC in the warm space improves the sealing effect of the curtain. The height of the opening itself was also tested, with works by Shih *et al.* (2011) [11], Moureh and Yataghene (2016) [12] and Gonçalves *et al.* (2019) [9]. The higher the opening, a higher initial jet velocity is needed to have optimal efficiency.

The effects of external parameters on the efficiency of an AC were also studied. The temperature difference between two spaces was studied by Gonçalves *et al.* (2019) [9], who concluded that the higher the temperature difference between spaces, the higher the initial jet velocity needed to obtain the maximum efficiency. As for the wind effect on air curtain performance, Yang *et al.* (2019) [13] found that wind action has negative impacts on the AC sealing effect, leading, in extreme cases, to the breakage of the jet. In these cases, the author recommended the usage of jets oriented to the outside to counter the effect of the wind flow. Finally, the effect of ventilation in buildings was tested by Siren (2003) [14] and Frank and Linden (2014) [15]. They concluded that the existence of

door or window openings in a building prevents the optimal functioning of an air curtain.

The performance of an air curtain can be calculated through experimental methods or numerical methods. In experimental methods, temperature sensors or the decay of concentration of a gas in a room (tracer gas technique) can be applied to calculate the efficiency of an AC. However, these methods can be expensive and time consuming, giving way to other approaches, for example, Computational Fluid Dynamics (CFD), a numerical computational method which enables 2D and 3D simulations. Many authors have tested this method with success, by comparing it with experimental results (Jaramillo *et al.* (2009) [8], Juraeva *et al.* (2011) [16], Foster *et al.* (2007) [17], Gonçalves *et al.* (2012b) [18] and Moureh e Yataghene (2017) [19]). However, there is still debate if 2D models are accurate. Works by Foster *et al.* (2007) [17] and Elicer-Cortés *et al.* (2009) [20] compared 2D and 3D results. While the first concluded that 2D models were not accurate, the second concluded that they provide similar results when compared to 3D models.

Being air curtains an expanding technology, this work intends to calculate the efficiency of an air curtain operating between two indoor spaces as the initial temperature difference between them changes. Secondly, it is intended to compute the efficiency of an air curtain between an indoor and an outdoor space as wind flow is increased. These tests will be performed with a CFD software, using 2D and 3D models, which will allow to evaluate if 2D models are as accurate as 3D models. The literature is scarce on the abovementioned objectives.

2. Methods

To achieve the abovementioned objectives, a CFD software (*Simcenter STAR-CCM+ 2019.2 Build 14.04.011*) was used to assess an air curtain efficiency at different temperature differences and wind flows. Validation studies were conducted first and case studies were then performed.

2.1 Validation studies

Validation studies consisted on the CFD modelling of a free turbulent plane jet. First, 2 computational domains (2D and 3D) were

implemented in order to test k-ε Standard, k-ε Realizable and LES (Large Eddy Simulation) CFD models. k-ε Standard and k-ε Realizable were tested in 2D geometry and LES in 3D geometry. The velocity profiles (centerline and transverse velocity profiles) of the modelled jets were used to validate the chosen model.

2.1.1 Computational domain, boundary conditions and jet parameters

As mentioned, a 2D and 3D domain were implemented. Their dimensions were $(L_x, L_y) = 13.5, 8$ m for the 2D domain and $(L_x, L_y, L_z) = 13.5, 8, 0.24$ m for the 3D one. For validation studies, all domain boundaries were considered as pressure outlets, with the exception of the jet nozzle plane (considered as a velocity inlet plane – width $H - 0.04$ m; velocity $U_0 - 3$ m/s; Reynolds number – 7692) and the lateral boundaries of the 3D domain (considered as symmetry planes).

2.1.2 Tests for mesh independence

Mesh independence tests were conducted in 2D geometry, for k-ε Standard and k-ε Realizable models, with three different mesh sizes: coarse grid (270400 cells), base grid (1080000 cells) and fine grid (2160000 cells). The results of jet velocity profiles are presented in Figure 1, showing mesh independence. Note that y is the distance from the jet centerline, U_y the velocity on distance y , U_c the jet centerline velocity and d the half-width of the jet.

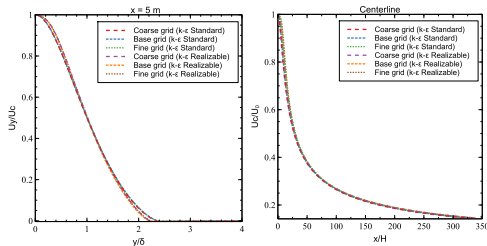


Figure 1 - Mesh independence for transverse jet velocity profile at $x=5$ m (left) and for jet centreline velocity (right)

Based on such results, the base grid (1080000 cells) was adopted.

2.1.3 Results for the validation studies

For the validation studies, the jet velocity profiles obtained in CFD and theoretical velocity profiles, experimental results (by Ramaprian *et al.* (1985) [21] and Deo *et al.* (2008) [22]) and DNS numerical results (by da Silva and Métais (2002) [23] and Stanley *et al.* (2002) [24]) were compared. As already mentioned, k-ε Standard

and k-ε Realizable models were tested in 2D geometry. LES model was tested in 3D geometry. The results of the validation studies are depicted in Figure 2:

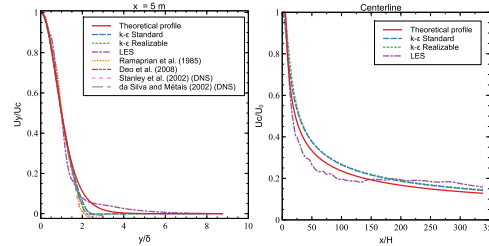


Figure 2 - Validation results for the transverse jet velocity profile at $x=5$ m (left) and for jet centerline velocity (right)

Although some differences between obtained results and theoretical, experimental and numerical data can be found, k-ε Realizable model is in good agreement. As such, it was selected for the case studies.

2.2 Case studies

The case studies consisted of three sets of tests: preliminary tests (in order to assess the proper functioning of the modelled air curtain); temperature tests and wind tests.

2.2.1 Computational domain

The computational domain for the case studies is presented in Figure 3. It was designed on SolidWorks (SolidWorks® Premium 2016 Edition), a Computer Aided Design (CAD) software, and then imported to Star-CCM+. As can be observed, it consisted of 2 rooms / spaces (width – 5 m, length – 5 m, height – 4 m) divided by a wall (0.3 m thick) with an opening (width – 1.5 m; height – 2 m). These dimensions were based on the recommendations from Eurovent [25], on the Commercial/Comfort category.

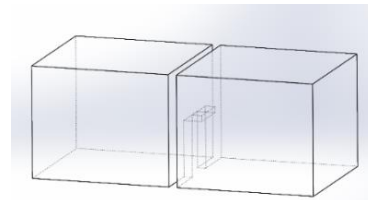


Figure 3 - Computational domain generated in Solidworks

2.2.2 Air curtain parameters

The jet selected for the case studies consisted of a jet designed in the warm room, with an initial velocity of 8 m/s, with a 0° orientation (vertical

jet). This was selected based on the parameters provided by a typical air curtain available on the market, by FRICO (PA2515A) [26], with a power of 161 W, a return grille of 1.5 x 0.16 m and a nozzle with 1.5 x 0.04 m, which resulted in a volumetric flow rate of 1728 m³/h (0.568 kg/s).

2.2.3 Boundary conditions

All surfaces on the computational domain were considered as adiabatic walls with the exception of the AC nozzle surface (velocity inlet plane) and the return grille surface (mass flow inlet plane). When the ACD was OFF, all its faces were considered adiabatic walls as well. The average temperature on the return grille surface was assigned to the nozzle surface. Some variations on the boundary conditions will be mentioned later.

2.2.4 Computational grid and physical models

The computational grid for the case studies consists on a grid with hexahedral elements with various dimensions. As for base dimensions, 8 cm cells were implemented. The grid was then gradually refined (with a rate of 50% compared with the previous one) when approaching to the area of the AC, resulting in cells with 1 cm (equal dimensions as the grid selected in the validation studies). This resulted in a 3D mesh with 4877057 cells (Figure 4).

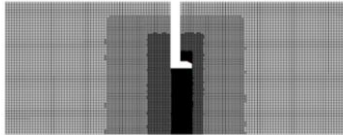


Figure 4 - Computational grid used in the case studies

In the case studies, the flow was modelled as incompressible, turbulent and unsteady, since the temperature evolution along the tests is of interest. The approach of segregated flow was used in all case studies. The Boussinesq approximation was used to model the non-isothermal cases. The fluid selected was air.

2.2.5 Preliminary tests

The air curtain was tested in 3 different, increasingly complex, isothermal tests, in order to assess the proper modelling of the domain and designed air curtain. These were 3 paired computational simulations (2D and 3D). The first preliminary test consisted only of a functioning nozzle, with lateral walls considered as pressure outlets. The second was similar to the first, but was added a functioning return grille. Finally, the

third one had adiabatic lateral walls, resulting in a closed domain, with a totally functioning AC and with the air curtain parameters and boundary conditions described.

2.2.6 Temperature tests (non-isothermal tests)

In order to evaluate the influence of temperature difference between rooms separated by an AC on its efficiency, 2D and 3D computational simulations, with and without AC, were conducted at different initial temperature differences (ΔT_i). The values used were based on the Eurovent recommendations [25], on the Commercial/Comfort category, and were 293 K for the warm room (room on the right), and 280, 275 and 266 K for the cold room, on the left ($\Delta T_i = 13, 18, 27$ K). As suggested by Eurovent, the simulations ended at $t = 60$ seconds, after which results were analysed.

2.2.7 Wind tests

In order to evaluate the influence of wind flow on the efficiency of an AC, 2D and 3D computational simulations, with and without AC, were conducted at different wind flows. 20 2D simulations were made, where 10 different wind flows were implemented (5 high wind flows and 5 low wind flows), with and without an AC. Also, 10 3D simulations were made, where 5 different wind flows were tested, with and without AC. In these, only $\Delta T_i = 18$ K was used. These were conducted in order to simulate 10 seconds of real time. As per recommendation of Eurovent [25], an exhaust duct (diameter of 0.4 m and length of 6 m) was added to the computational domain. It was installed in the warm room, on the wall furthest from the opening, aligned with it, and considered as a negative mass flow inlet surface. This simulates the presence of wind flow through the opening. As for the boundaries described before, an alteration was implemented in wind tests: the surface located furthest from the opening in the cold room was considered as a pressure outlet, simulating the exterior. Moreover, 2 pairs of planes, located at 0.17 m and 0.55 m of the opening were designed in each space. These allowed to calculate a pressure difference (Δp) between spaces using a surface integral. Since Eurovent recommends a Δp between 0.5 and 8 Pa, the wind flows used were as followed:

- 2D low wind flows: 0.5, 0.75, 1, 1.25 and 1.5 kg/s or 0.42, 0.63, 0.84, 1.06 and 1.25 m³/s
- 2D high wind flows: 5, 5.5, 6, 7 and 8 kg/s or 4.22, 4.65, 5.07, 5.91 and 6.76 m³/s

- 3D wind flows: 2.5, 3, 4, 5 and 6 kg/s or 2.11, 2.53, 3.38, 4.22 and 5.07 m³/s

Results were then analysed.

2.3 Sealing efficiency of an air curtain

The sealing efficiency (η_Q) of an air curtain is defined as the ratio between the reduction of the energy (or power) transferred with the ACD ON and the transfer of energy (or power) with the ACD OFF [10] (Equation (1)):

$$\eta_Q = 1 - \frac{Q_{AC}}{Q_{noAC}} \quad (1)$$

where Q_{AC} (kW) is the heat loss through the opening with the ACD ON and Q_{noAC} (kW) is the heat loss through the opening with the ACD OFF.

As recommended by Eurovent, the power of the air curtain device was added to Equation (1) resulting in Equation (2):

$$\eta_Q = 1 - \frac{Q_{AC} + P_e}{Q_{noAC}} \quad (2)$$

where P_e (kW) is the power of the ACD.

For the wind tests, Eurovent also suggests the infiltration efficiency (η) (Equation (3)), when the door is subjected to the same pressure difference with and without AC:

$$\eta = 1 - \frac{q_{AC}}{q_{noAC}} \quad (3)$$

where q_{AC} (m³/s) is the volumetric flow rate through the opening with the presence of an AC and q_{noAC} (m³/s) is the volumetric flow rate through the opening with the absence of an AC.

In order to calculate the heat loss through the opening, Eurovent provides the following Equations (4) (used for the temperature tests) and (5) (used for the wind tests):

$$Q(kW) = \frac{V\rho c_p(T_i - T_f)}{\Delta t} \quad (4)$$

$$Q(kW) = \frac{q_{@2.5Pa}\rho c_p(T_i - T_f)}{\Delta t} \quad (5)$$

where V (m³) is the volume of the room, ρ (kg/m³) is the density of the air in the room, c_p (kJ/kgK) is the specific heat of the air in the room, T_i is the temperature in the room at instant t_i , T_f is the temperature in the room at instant t_f , $\Delta t=(t_f-t_i)$ is the duration of the test and $q_{@2.5Pa}$ the

volumetric flow rate measured in the exhaust duct at a pressure difference of 2.5 Pa.

3. Results and Discussion

3.1 Preliminary tests results

2D and 3D paired preliminary tests showed the jet decay and spreading rates presented in Figure 5, which are characteristic of a well modelled free turbulent plane jet. As observed, results for preliminary test 3 in 2D differs from the others. Note that y is the distance from the AC jet inlet.

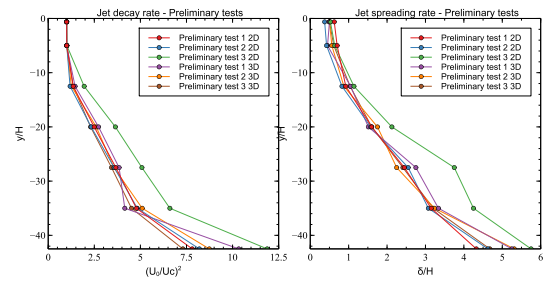


Figure 5 - Jet decay (left) and spreading (right) rates - Preliminary tests

When adiabatic lateral walls (preliminary test 3) were included, the jet showed a deflection to the return grille, which was more accentuated in the 2D case (Figure 6). This can be justified by the fact that, in a 2D model, the dividing walls and the gradients in the z direction are not accounted, and the pressure imposed on the jet is distributed by 2 dimensions only.

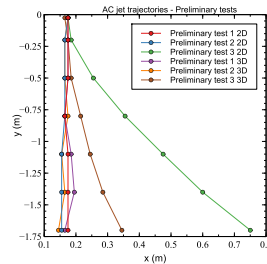


Figure 6 - Jet trajectories - Preliminary tests

3.2 Temperature Tests

All figures presented refer to $\Delta T_i = 18$ K. Results obtained with $\Delta T_i = 13, 27$ K are similar for the following sections.

3.2.1 Jet spreading and jet decay rates

The jet spreading and decay rates showed well modelled free turbulent plane jets. No significant differences were obtained at the 3 different ΔT_i .

3.2.2 Velocity fields and jet trajectories

The velocity fields presented in Figure 7, show that for both 2D and 3D cases, with the ACD ON, the jet deflects to the warm room, where the return grille is installed. The grille creates a negative pressure in the warm room, more prominent for 2D cases, resulting in a higher jet deflection and more evident air circulation in 2D geometry.

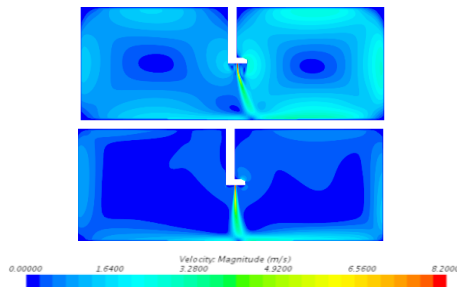


Figure 7 - Velocity fields for the temperature tests with AC at 60 s, $\Delta T_i=18$ K, 2D (above) and 3D (below)

With the ACD OFF (Figure 8), a region with a higher velocity value in the upper area of the cold room can be observed. This is due to natural convection. The neutral level described by Emswiler [27] can also be seen. This was more prominent in 3D cases.

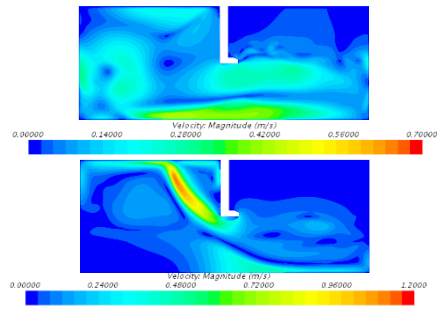


Figure 8 - Velocity fields for the temperature test without AC at 60 s, $\Delta T_i=18$ K, 2D (above) and 3D (below)

3.2.3 Temperature fields

With the ACD ON, for both 2D and 3D cases, a barrier between the two rooms was clearly seen. This corresponded to the jet produced. Specifically, for the 2D cases, the center of each room maintained its temperature during the 60 s, evidence of the circulation of air in the periphery of the rooms (Figure 9). This is in accordance with the velocity field shown in Figure 7.

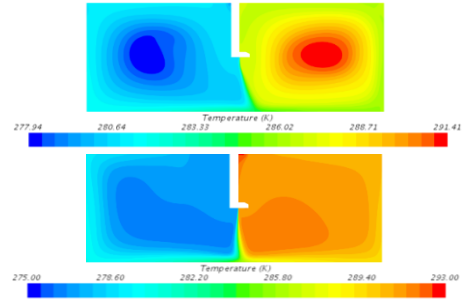


Figure 9 - Temperature fields for the temperature tests with AC at 60 s, $\Delta T_i=18$ K, 2D (above) and 3D (below)

With the ACD OFF, for the 2D and 3D cases, 3 distinct masses of air are seen (Figure 10). For the 3D cases, as observed in the velocity fields (Figure 8), natural convection is clearly seen.

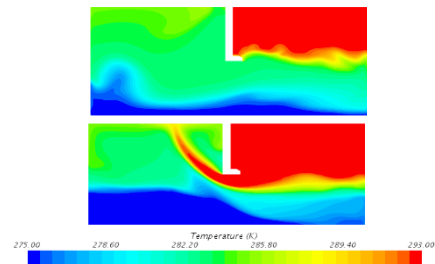


Figure 10 - Temperature fields for the temperature test without AC at 60 s, $\Delta T_i=18$ K, 2D (above) and 3D (below)

3.2.4 Temperature evolution throughout the simulations

In Figure 11, the temperature evolutions in each room are presented for 2D and 3D when the ACD is ON and OFF. It can be concluded that the AC dampens heat transfer. The temperature differential in each room was lower with the presence of an air curtain.

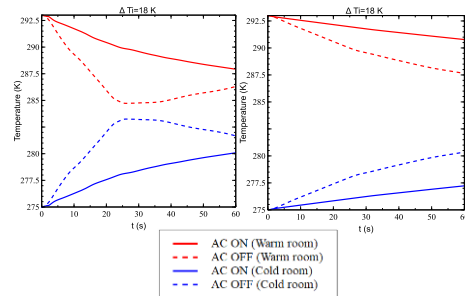


Figure 11 - Temperature evolution on each room with $\Delta T_i=18$ K, 2D (left) and 3D (right)

For the 2D cases, with the ACD OFF, it is noticeable that during the 60 seconds, the warm room experienced both heat loss and heat gain. This phenomenon observed in the 2D cases with the ACD OFF does not occur in their 3D counterparts, due to the fact that in the 3D

geometry, the two rooms are separated by walls, which hamper the return of the warm air to the warm room.

3.2.5 ΔT_i influence on the AC sealing efficiency

The sealing efficiency of the AC for each case is presented in the Table 1 and the relation between the ΔT_i and the sealing efficiency is observed in Figure 12.

Table 1 - Sealing efficiency of the AC for the temperature tests

Sealing efficiency (%)	2D	3D
13 K	22	52
18 K	18.2	57
27 K	10.8	61.5

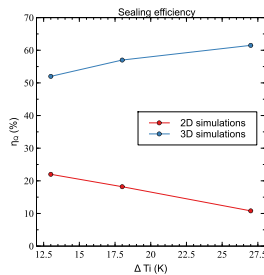


Figure 12 - Sealing efficiency evolution with ΔT_i

The efficiencies obtained in the 3D cases are significantly higher than the ones obtained in the 2D cases. This can be attributed to the fact that in the 3D cases the restricting effects of the dividing walls are present, whereas in the 2D cases, this does not happen. Thus, there is a proportionally higher heat and mass transfer in the 2D cases.

In addition, the results between the 2D and 3D cases showed different tendencies: in the 3D cases, the sealing efficiency increases when the ΔT_i increases whereas in the 2D the opposite occurs. The results found in the 3D cases, are in good agreement with the results by Gonçalves *et al.* [9]. Since 3D simulations are closer to a real scenario and the fact that the 3D cases exhibit dissimilar results from the 2D ones, it can be concluded that the latter is not well suited when testing an AC.

Thus, it is concluded that:

- The sealing efficiency of an AC increases with the increase of ΔT_i ;
- 2D simulations are not reliable when testing an air curtain.

3.3 Wind Tests

3.3.1 Evolution of the pressure difference across the opening with the wind volumetric flow

In Figure 13, the pressure differences between rooms, across the opening, and their respective volumetric flows, can be observed for the 2D cases (high and low wind flow ranges) and the 3D cases, with the ACD ON and OFF. These were measured at 0.55 m. The pressure differences at 0.17 m have similar trends.

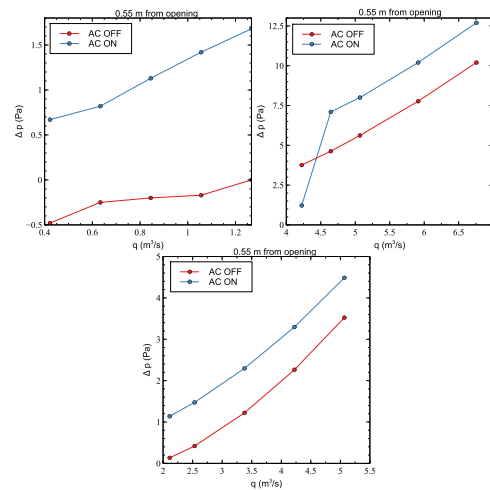


Figure 13 - Δp vs q , for the 2D wind tests (above) and 3D wind tests (below). 2D low flows on the left and 2D high flows on the right.

It was observed that, as expected, higher wind flows correspond to higher pressure differences across the opening. Moreover, with the ACD ON, pressure differences across the opening are higher when compared with the ACD OFF. When the ACD is ON, a resistance to air flow is created, which means that, for a certain air flow, a higher pressure difference occurs (Ohm's Law, applied to Fluid Mechanics).

Only for 2D low range air flows with the ACD OFF, negative values of pressure difference were obtained across the opening, justified by the fact that natural convection overpowered the air flow imposed, resulting in the escape of warm air to the exterior.

An unexpected deflection of the AC jet occurred in one test: 2D case with $q = 4.22 \text{ m}^3/\text{s}$ (5 kg/s). This led to an absence of an effective air curtain and explains the sudden decrease in pressure difference observed in Figure 13 (2D high range flows). The reason for this occurrence is not clear, but reinforces disadvantages in 2D CFD simulations.

3.3.2 Velocity fields

In Figure 14, the velocity field for the case of $5.07 \text{ m}^3/\text{s}$ in 2D (middle value of the high range and representative for this range) is presented. There was no significant difference between the case with and without the AC. The jet never reached the floor, since it was overpowered by such high air flows. These results are in agreement with Yang *et al.* [13]. This was not observed for the low flows in 2D and the wind flows in 3D, where the jet was not overpowered (Figure 15). However, the jet was still deflected. The higher the air flow, the bigger the deflection.

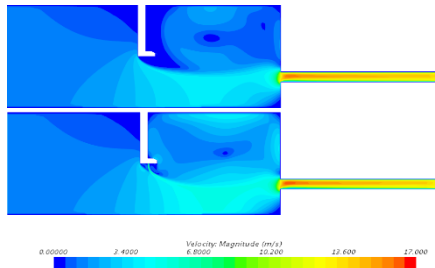


Figure 14 - Velocity fields for the wind test for $5.07 \text{ m}^3/\text{s}$ (6 kg/s) at 10 s , without AC (above), with AC (below), 2D

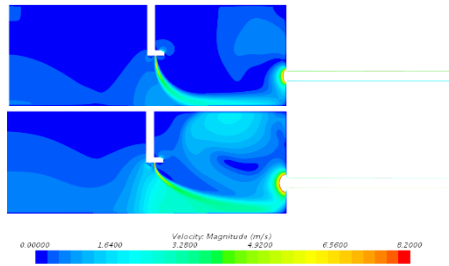


Figure 15 - Velocity fields for the wind test for $2.11 \text{ m}^3/\text{s}$ (2.5 kg/s) (above) and $5.07 \text{ m}^3/\text{s}$ (6 kg/s) (below) at 10 s , with AC, 3D

The effects of the dividing walls in the top views of the 3D cases (Figure 16) show the Coanda Effect, which is not present in 2D cases and further explains why 2D are not suitable for AC CFD studies.

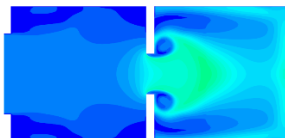


Figure 16 - Velocity field (top view) for the wind test for $5.07 \text{ m}^3/\text{s}$ (6 kg/s) at 10 s , with AC, 3D

3.3.3 Final temperatures in the warm room

The final temperatures with or without the AC in the warm room exhibit no significant differences. This is due to the fact that the same air flows are imposed with and without the AC. As expected,

as air flow is increased, the final temperature in the warm room is lower. In the exterior, the temperatures remained fairly constant during the 10 seconds (275 K) (Table 2 and Table 3).

Table 2 - Final temperatures (at 10 s) in the warm space for the 2D cases

2D	\dot{m} (kg/s)	q (m^3/s)	Tf without AC (K)	Tf with AC (K)
Low flows	0.5	0.42	287.4	289.7
	0.75	0.63	287.5	288.5
	1	0.84	287.4	287.4
	1.25	1.06	286.8	286.6
	1.5	1.27	286.0	285.2
High flows	5	4.22	281.4	275.3
	5.5	4.65	281.2	280.4
	6	5.07	281.0	280.8
	7	5.91	280.7	280.8
8	6.76	280.3	280.6	

Table 3 - Final temperatures (at 10 s) in the warm space for the 3D cases

\dot{m} (kg/s)	q (m^3/s)	Tf without AC (K)	Tf with AC (K)
2.5	2.11	289.6	289.7
3	2.53	289.1	289.1
4	3.38	288.3	288.2
5	4.22	287.6	287.3
6	5.07	287.0	286.4

3.3.4 Δp influence on the AC sealing efficiency

In Table 4, Table 5 and Figure 17, the evolution of the sealing and infiltration efficiencies with the pressure difference across the opening are presented both for the 2D and 3D cases. These efficiencies were calculated for 3 different pressure differences: 1 Pa , 2.5 Pa (recommended by Eurovent) and 4 Pa (used by Sherman and Grimsrud (1980) [28] as a reference value in the USA). These were also calculated for the 2 pairs of planes at a distance of 0.17 m and 0.55 m from the opening, using equations (5) and (2).

Table 4 - Sealing and infiltration efficiency of the AC for planes at 0.17 m from the opening for 2D and 3D cases

Sealing efficiency (%) / Infiltration efficiency (%) 0.17 m from the opening	2D	3D
1 Pa	16.1 / 25	42 / 35.6
2.5 Pa	4.9 / 13.6	18 / 16.8
4 Pa	0 / 8.8	6.5 / 10

Table 5 - Sealing and infiltration efficiency of the AC for planes at 0.55 m from the opening for 2D and 3D cases

Sealing efficiency (%) / Infiltration efficiency (%) 0.55 m from the opening	2D	3D
1 Pa	35 / 42.4	46.5 / 39.3
2.5 Pa	25.2 / 29.9	21.4 / 19
4 Pa	21.5 / 24.3	9 / 11.4

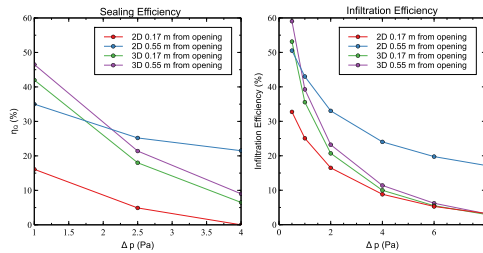


Figure 17 - Sealing and Infiltration efficiency vs Δp in the opening

Analysing the graphs, it can be observed that both 2D and 3D results exhibit the same trends: the bigger the pressure difference across the opening, the lower the sealing and infiltration efficiency of the AC. Also, both the sealing and infiltration efficiency are higher when the pressure difference is measured in the pair of planes at 0.55 m from the opening.

When comparing the 2D and 3D results, similarly to what happened in the temperature tests, these showed different results.

As said in 3.2.5, 3D results were deemed more reliable. They represent more accurately the real geometry of the spaces. Moreover, when conducting the 2D simulations, as already mentioned, an unexpected deflection of the jet for air flows between 2 kg/s and 5 kg/s was observed. This precluded direct assessment of pressure differences of 1 to 4 Pa across the opening at such air flows. So, a linear regression on Δp vs q graphs was used to obtain these pressure differences. This may have brought some errors to the final results in the 2D geometry.

Thus, after the wind tests and results were analysed, it is inferred that:

- The efficiency of the air curtain decreases when there is a bigger pressure difference across the opening (higher air flow passing through the opening, or higher wind flows);
- As seen in the temperature tests, the 2D models are not reliable.

3.4 2D vs 3D simulations

One of the objectives of this work was to analyse the differences between the 2D and 3D simulations and to assess if the 2D simulations, which are computationally less demanding, are a good representation of air curtain testing. As already concluded in 3.2.5 and 3.3.4, the use of 2D geometries when evaluating the performance

of an air curtain has some disadvantages. They are not a reliable mean of representing 3D spaces. Therefore, the use of 3D models for air curtain testing is highly recommended to obtain more accurate results.

4. Conclusions and Future work

4.1 Conclusions

The main goals of this work were to evaluate how temperature differences and wind flows (pressure differences across the opening) impacted on the sealing efficiency of an air curtain. In order to achieve such goals, CFD simulations were conducted in Star-CCM+, in 2D and 3D domains.

On temperature differences, it was concluded that the bigger the initial temperature difference between spaces, the higher the AC efficiency. This was observed for the 3D cases. However, the 2D tests showed an opposite trend, thus showing that they are not a reliable method of studying an air curtain in CFD.

On wind flows, it was concluded that, when the wind air flow (or the pressure difference across the opening) increases, the sealing efficiency of the AC decreases. This trend was observed both in 2D and 3D cases. However, these showed different results once again, reinforcing that 2D CFD simulations are not suitable for AC studies.

4.2 Future work

To further improve the knowledge on air curtains, additional work can be done. First, to confirm the results obtained in CFD, experimental tests based on the initial conditions used in this work should be conducted. Secondly, the use of other air curtain and room parameters, (jet orientation, velocity, inlet dimensions, other initial temperature differences, room dimensions and other wind air flows) would be useful to amplify the results obtained. Finally, since this study showed that 2D is not reliable and there is still debate about its accuracy, it is recommended that air curtain testing using CFD should be conducted in 3D domains.

Bibliography

1. Howell RH, Shibata M. Optimum heat

- transfer through turbulent recirculated plane air curtains. *ASHRAE Transactions*. 1980;86 (1): 188–200.
2. Zion Market Research - “Europe Air Curtain Market (Re-Circulating Air Curtains and Non Re-Circulating) For Commercial, Industrial And Others: Europe Industry Perspective, Comprehensive Analysis, and Forecast, 2016 – 2022”. 2017.
 3. Takahashi K, Inoh M. Some measurements on air curtain efficiency for cold rooms. In: *Proc. 11th International Congress of Refrigeration*. 1963; Vol. II:1035–1039.
 4. Hayes FC, Stoecker WF. Design data for air curtains. *ASHRAE Transactions*. 1969; 75 (2):168–180.
 5. Hayes FC, Stoecker WF. Heat transfer characteristics of the air curtain. *ASHRAE Transactions*. 1969;75 (2): 153–167.
 6. Costa JJ, Oliveira LA, Silva MCG. Energy savings by aerodynamic sealing with a downward-blowing plane air curtain-A numerical approach. *Energy Build*. 2006;38(10):1182–93.
 7. Paepe M. Study of air curtains used to restrict infiltration into refrigerated rooms. *Int Conf on Heat Transf Fluid Mech and Thermo*. 2010; 1763-69.
 8. Jaramillo JE, Pérez-Segarra CD, Oliva A, Olliet C. Analysis of the dynamic behavior of refrigerated spaces using air curtains. *Numer Heat Transf Part A Appl*. 2009;55(6):553–73.
 9. Gonçalves JC, Costa JJ, Lopes AMG. Parametric study on the performance of an air curtain based on CFD simulations - New proposal for automatic operation. *J Wind Eng Ind Aerodyn*. 2019;193:103951.
 10. Gonçalves JC, Costa JJ, Figueiredo AR, Lopes AMG. CFD modelling of aerodynamic sealing by vertical and horizontal air curtains. *Energy Build*. 2012;52:153–60.
 11. Shih YC, Yang AS, Lu CW. Using air curtain to control pollutant spreading for emergency management in a cleanroom. *Build Environ*. 2011;46(5):1104–14.
 12. Moureh J, Yataghene M. Numerical and experimental study of airflow patterns and global exchanges through an air curtain subjected to external lateral flow. *Exp Therm Fluid Sci*. 2016;74:308–23.
 13. Yang S, Alrawashdeh H, Zhang C, Qi D, Wang L, Stathopoulos T. Wind effects on air curtain performance at building entrances. *Build Environ*. 2019;151:75–87.
 14. Sirén K. Technical dimensioning of a vertically upwards-blowing air curtain - Part II. *Energy Build*. 2003;35(7):697–705.
 15. Frank D, Linden PF. The effectiveness of an air curtain in the doorway of a ventilated building. *J Fluid Mech*. 2014;756:130–64.
 16. Juraeva M, Lee J ho, Song DJ. A computational analysis of the train-wind to identify the best position for the air-curtain installation. *J Wind Eng Ind Aerodyn*. 2011;99(5):554–9.
 17. Foster AM, Swain MJ, Barrett R, D’Agaro P, Ketteringham LP, James SJ. Three-dimensional effects of an air curtain used to restrict cold room infiltration. *Appl Math Model*. 2007;31(6):1109–23.
 18. Gonçalves JC, Costa JJ, Figueiredo AR, Lopes AMG. Study of the aerodynamic sealing of a cold store - Experimental and numerical approaches. *Energy Build*. 2012;55:779–89.
 19. Moureh J, Yataghene M. Large-eddy simulation of an air curtain confining a cavity and subjected to an external lateral flow. *Comput Fluids*. 2017;152:134–56.
 20. Elicer-Cortés JC, Demarco R, Valencia A, Pavageau M. Heat confinement in tunnels between two double-stream twin-jet air curtains. *Int Commun Heat Mass Transf*. 2009;36(5):438–44.
 21. Ramaprian BR, Chandrasekhara MS. LDA measurements in plane turbulent jets. *J. Fluids Eng*. 1985;107: 264-271.
 22. Deo RC, Mi J, Nathan GJ. The influence of Reynolds number on a plane jet. *Phys Fluids*. 2008;20(7).
 23. da Silva CB, Métais O. On the influence of coherent structures upon interscale interactions in turbulent plane jets. *J Fluid Mech*. 2002;473(473):103–45.
 24. Stanley SA, Sarkar S, Mellado JP. A study of the flow-field evolution and mixing in a planar turbulent jet using direct numerical simulation. *J Fluid Mech*. 2002;450:377–407.
 25. Eurovent. Air curtain unit - Classification , test conditions and energy performance calculations. 2016. Vol. 32. 1–35 p.
 26. FRICO PA2500. FRICO website, <https://shop.frico.net/en/pa2500/c45356>, visited on 5th November 2020.
 27. Emswiler JE. *Journal of the American Society of Heating and Ventilation Engineers*. 1926;32 (1):1-16.
 28. Sherman MH, Grimsrud D. Infiltration-pressurization correlation : Simplified physical modeling. 1980.